Indian Journal of Chemistry
Vol. 62, October 2023, pp. 1001-1011
DOI: 10.56042/ijc.v62i10.1578

De-Novo drug design of novel 1,2,3–triazole-naphthamide as an inhibitor of SARS-Cov-2 main protease: Synthesis, bioinformatics and biophysical studies

Sourav Misra[a], Sandip Paul[a,c], Sourav Pakrashy[a,b], Sayan Ghosh[a], Susmita Naskar[a], Pawan Kumar Maurya[b], Pinki Saha Sardar[c], Katta Venkateswarlu[d], Adity Bose[a] & Anjoy Majhi*[a]

[a] Department of Chemistry, Presidency University, 86/1 College Street, Kolkata 700 073, India

[b] Indian Council of Medical Research-Centre for Ageing and Mental Health, Division of Non-Communicable Diseases, Kolkata 700 091, India

[c] Department of Chemistry, The Bhawanipur Education Society College, Kolkata 700 020, India

[d] Department of Chemistry, Yogi Vemana University, Kadapa 516 005, Andhra Pradesh, India

E-mail: anjoy.chem@presiuniv.ac.in; adity.chem@presiuniv.ac.in

Received 19 May 2023; accepted(revised) 20 September 2023

A novel 1,2,3-triazole-napthamide molecule (SSAM-1) is designed as per De-Novo drug design method and synthesized by using copper-catalyzed alkyne-azide cycloaddition reaction. The interaction studies of SSAM-1 with bovine serum albumin (BSA), human serum albumin (HSA) and bromelain (BMLN) are investigated by steady state fluorescence spectroscopic studies. The experimental results for these interaction studies are validated by molecular docking method. The theoretical prediction of ADMET properties of SSAM-1 are also performed using computational methods. All these studies indicate significant and spontaneous binding of SSAM-1 with serum albumins and BMLN at *p*H 7 under varying temperature conditions (288K, 298K, 308K). In all the three cases the interaction of the molecule with the proteins and enzymes led to quenching of the fluorescence emission (mainly *via* static quenching mechanism) of tryptophan (Trp) residue present in the proteins and in the enzyme. The complexation with SSAM-1 changes the microenvironment of the Trp residue(s) of BSA, HSA and BMLN. Strong binding affinity between proteins and SSAM-1 is indicated by the binding constant values, which is in 10^3-10^5 orders. Hydrophobic forces are acting as the major interacting forces for SSAM-1-HSA interaction while H-bonding and van der Waals forces are acting as the primary interacting forces for SSAM-1 interacting with BSA and BMLN. ADMET prediction reveals the drug-able nature of SSAM-1 which is justified due to its ability to bind with the serum albumins. In addition binding study of SSAM-1 with BMLN indicates its possibility of oral administration. Conducting such binding studies of the newly synthesized triazole with biomolecules, an effort is made to assess the contribution of a novel compound to the development of medicines for the drug design process at a very early stage of the research.

Keywords: Triazole, Click Reaction, Binding Interaction, Drug design, Docking, ADMET prediction

In De-Novo designs, we tend to discover a new chemical entity that sits at the active site of the target protein, receptor or enzyme[1]. It starts by exploiting an existing moiety and we keep modifying it by adding or subtracting fragments step-by-step, so that may be when a particular group is added, it increases the electrostatic interaction or it improves the hydrophobic interaction or it produces a good hydrogen bond donor or it reduces steric repulsion or van der Waals repulsion. Assembling of the novel moieties from pieces that are positioned optimally in favourable regions of the active site we create a new scaffold or drug candidate which probably shows very good interaction. Here, after designing the new structure we run the docking protocol against our targeted protein, checked score and compared with the dock score of the existing moiety[2]. When found that our newly designed molecule showed better docking score (ΔG value), we synthesized it to explore its medicinal properties.

Serum albumins are the main carrier of endogenous and exogenous compounds in the blood stream. The most popular serum albumins, bovine serum albumin (BSA) and human serum albumin (HSA), are essential components of numerous biological systems[3,4]. The molecular weight of these two serum albumins (SA) is nearly identical (66 KDa and 66.5 KDa for BSA and HSA, respectively), and they have nearly 80% structural similarity[5]. The aromatic amino acids tryptophan (Trp), tyrosine (Tyr), and phenylalanine (Phe) are found in proteins and can exhibit intrinsic fluorescence of proteins. Trp is the

amino acid in proteins that is most frequently employed for fluorescence analysis[6,7]. Studying protein-ligand interactions is crucial for building new systems and designing drugs. At the initial stage of research, protein ligand binding studies tell us whether a ligand (molecule/compound) may operate as a medication or not[5,6].

Bromelain (BMLN) derived from stem of pineapple is an enzyme of proteolytic nature having molecular weight of 23.40-35.73 kDa, containing a total of 285 amino acids with 8 tryptophan residues[8].Effect of *Vibrio cholera* and *E. coli* which are mainly intestinal pathogens are prevented by BMLN, these pathogens releases enterotoxins which is responsible for causing diarrhoea, some studies suggested anti-adhesive effects[9] of BMLN which prevents bacteria to attach to specific glycoprotein receptors situated on intestinal mucosa by proteolytically modifying the receptor attachment regions used during the *E. coli* infection[10].Some studies indicate that BMLN can act as a drug carrier which makes the drug molecule suitable for oral administration[11]. Thus we can predict that if any moiety which can bind with a good score with BMLN may have anti-bacterial effects and can prevent bacterial colonisation by binding with specific glycoproteins. In addition, binding of a potential drug candidate with BMLN can be considered as its possibility of oral administration.

The current research mainly involves designing and synthesis of novel triazole-naphthamide, SSAM-1 (Fig. 1) and study of its interaction with BSA, HSA and BMLN. The designing is done in accordance to De-novo drug design method.The synthesis is carried out using "click chemistry" also known as the Cu(I)-catalyzed cycloaddition of alkyne and azide (CuAAC) reaction which easily produces 1,2,3-triazole moiety[12,13], which was first developed by Sharpless and it is one of the most significant methods for cycloaddition reactions. The interaction studies were carried out utilising fluorescence spectroscopyy and molecular docking techniques. A number of 1,2,3-triazole-based derivatives were previously synthesised[14,15] via the CuAAC process[16] and

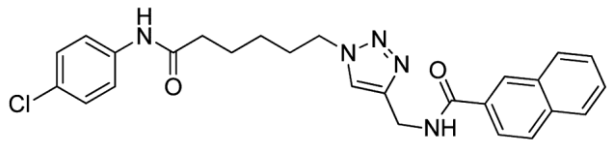

Fig. 1 — Chemical structure of SSAM-1

demonstrated a variety of applications[15] including medicines.[17] These compounds are now commercially available as medications.

Thereby conducting binding studies of the newly synthesized compound with biomolecules, an effort is made to assess the contribution of a novel compound to the development of biomedicines for the drug design process at a very early stage of the research.

Materials and Methods

General information

The steady state emission measurements of serum albumins with varying concentrations of SSAM-1 were carried out using a Hitachi Model F-4700 spectrofluorimeter equipped with a 150 W xenon lamp, at 298 K using a stopper cell of 1 cm path length. The stock solutions of serum albumins (BSA/ HSA) are prepared in phosphate buffer (pH7). The concentration of both the serum albumins for the experiments kept at 10μM in phosphate buffer (pH7). The steady state fluorescence emission studies have been carried out with addition of varying concentrations of SSAM-1 upon 10μM serum albumins at 298K.

^{1}H and ^{13}C NMR spectra were recorded on AVANCE 400 MHz FT-NMR spectrometer, at operational frequency of 400 MHz and 100 MHz respectively, Bruker Biospin AG using Dimethyl sulfoxide-d_6 ($(CD_3)_2SO$)) containing 0.05% tetramethylsilane (TMS) (99.8%D, Cambridge Isotope Laboratories, Inc., Cat. No. DLM-7, 13K-471).

In-Silico Docking Analysis

The in-silico screening of the compounds, that is, docking analysis of proteins with different ligands was assisted by UCSF Chimera, Auto-Dock-Vina[18] (the program was carried out as an add-on in UCSF Chimera) to study the interaction affinity between Triazole-naphthamide and the main protease (M^{pro}) of SARS-CoV-2.

The M^{pro} protein was taken from Protein databank (RCSB PDB), 6LU7 (PDB-ID) in PDB format. Prior to in-silico studies, water molecules and other solvent molecules and the co-crystallized residue, were removed using UCSF-Chimera. Preparation of the structure of protein was then prepared using Dock Prep tool by writing the hydrogen atoms, specific charges and steps for minimization of total energy of protein[19]. AM1-BCC method assigned the charges which are quick and efficient for the generation of high-quality charges of atom for protein and the

ANTECHAMBER algorithm[20] helps in computation of charges. Seven-hundred (700) steepest descent steps with 0.02 Å step size for the energy minimization of the protein was performed with an update interval of ten (10) and saved in PDB format. All these were performed using UCSF-Chimera. The protein energy minimization was further done with Swiss PDB viewer[21].

For *in-silico* interaction assay with SSAM-1, its structure was drawn in chemdraw, these drawn structures were copied and pasted to software Chem3D pro where its minimization of energy was carried using MM2 calculations, after that it was saved in SDF format. Now before carrying out the molecular docking the ligand is optimized by addition of hydrogen and addition of charge using Gasteiger algorithm,[22] energy minimization was performed using nine hundred (900) steepest descent steps with step size of 0.02 Å with an update interval of ten (10) in the structure editing wizard of UCSF-Chimera and then again saved in PDB format, which works on the principle of chemoinformatics of electronegativity equilibration. A grid box which assigns the binding region was chosen in such a way that it would cover the specific binding site for the hydrophobic surface of the concave region of protein. To fit in properly the hydrophobic surface of the ligand giving the best binding score.

Molecular docking of our designed moiety was further done with BSA, HSA and BMLN. In order to do so we retrieved the proteins X-ray crystallographic structure in PDB format from RCSB PDB website (http://www.rcsb.org/pdb) bearing PDB ID's 4F5S (BSA) and 1AO6 (HSA), but X-ray crystallographic structure in PDB format is unavailable in the website, so we took 1W0Q (BMLN) which is a formed structure through homology modelling. This modelled protein showed good result according to the positions occupied by its residues in Ramachandran Plot (Figure S1). Thus we used the PDB format of 1W0Q to dock with our designed moiety. All other steps involving protein preparation, ligand preparation and other necessary ones for docking protocol[2] are kept same as stated above. For visualising in many formats we used software's UCSF-Chimera and Discovery studio.

ADMET Analysis

To investigate the physicochemical properties of the secondary metabolites of all the plants, In-silico ADMET analysis was done, these are water solubility, lipophilicity and pharmacokinetics and performed by using following website http://www.swissadme.ch,[23] but the toxicity of these molecules cannot be investigated by using Swiss ADME, so help was taken from pkCSM[24] - pharmacokinetics server to predict the Toxicity along with other ADME parameters of the molecules with their SMILE (Simplified Molecule Input Line Entry Specification) profile.

Results and Discussion

De novo Drug Design

De novo means starting from the scratch. So we start by gathering the knowledge of the structure of the binding site to understand the major interactions by downloading the X-ray crystallography structure of the target protein with a bound ligand from RCSB PDB website. In this case, it is the Covid 19's chymotrypsin protein or the main protease (M^{pro}) bearing PDB ID: 6LU7. The bound ligand which is a covalent inhibitor formed by amide coupling with several amino acids and we thrive to lower the labour by changing site with a bioisostere and keeping intact the three nitrogen atoms of the three amide bond. Then we systematically start building these binding areas with aromatic ring or a carbonyl or a heterocyclic fragment and all of these are designed according to the specific residues at the active site of protein. Now we just bridge these molecules to get a new structure which is going to perhaps show better activity (Fig. 2).

To understand the interactions, we use a software known as LIGPLUS to get the knowledge of the binding residues and bonding of the co-crystallized ligand with the target protein at its binding site (Figure S2 in SI).

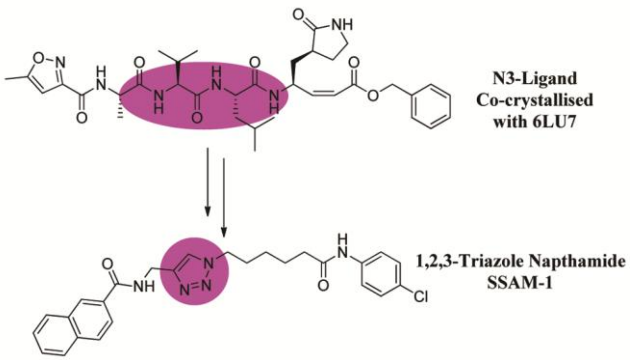

Fig. 2 — Evolution of 1, 2, 3- triazole-naphthamide (SSAM-1) via de novo drug design

Results of Docking

The binding interactions between the targeted protein 6LU7 (PDB-ID) and the ligands which are mainly the co-crystalized ligand N3 (PubChem ID – 146025593), Molnupiravir an anti-viral drug (PubChem ID – 145996610) and our designed ligand SSAM-1 are found out using molecular docking using the free and effective software Auto-Dock-Vina. The calculations unfold the free energy change for these interactions as ΔG = - 6.9, -6.8 and -7.9 kcal/mol respectively (Table 1). Grid box for our Protein M^{pro} 6LU7 taken as -11 × 12 × 69Å with size 30 × 30 × 30 Å along x-, y- and z- axes. Our newly designed moiety SSAM-1 showed better protein ligand binding interactions with the targeted protein 6LU7 than its co-crystallized ligand and a known anti-viral drug Molnupiravir.

The binding region of SSAM-1 shown in Figure S3 (SI), and the other docking poses including 2D diagram, H-bonding zone and protein active site bound are given in Fig. 3.

In-silico binding studies of our designed moiety with BSA (PDB ID - 4F5S), HSA (PDB ID - 1AO6) and BMLN (PDB ID - 1W0Q) revealed that ΔG value for these interactions to be sufficient to become a drug candidate. Grid box for BSA protein was taken as 64× 24 × 29 Å with size 136 × 64 × 94 Å along x- , y- and z- axes and ΔG value of - 10.8 kcal/mol, grid box for HSA protein was taken as 28.32 × 8.11 × 21.48 Å with size 78.78 × 102.33 × 75.37 Å along x- , y- and z- axes and ΔG value of - 9.4 kcal/mol and grid box for BMLN was taken as - 2.6 × 4.2 × - 0.75 Å with size 51 × 36 × 36 Å along x- , y- and z- axes and ΔG value of -10.2 kcal/mol (Table 2). The docking poses upholds the importance of triazole region as it gets primarily involved in the formation of either strong hydrogen bond or amide pi-stacking or pi-sigma bond formation respectively, with proteins BSA, HSA and enzyme BMLN (Fig. 4, Fig. 5 and Fig. 6).

Table 1 — Results of the Docking of N3 ligand, Molnupiravir and SSAM-1 with 6LU7

Name	PubChem ID	Docking Score (kcal/mol) 6LU7
N3 Ligand	146025593	-6.9
Molnupiravir	145996610	-6.8
SSAM-1	--	-7.9

Synthesis of SSAM-1

Our designed compound SSAM-1 was prepared according to procedure in the literature[5] and the retro synthetic pathway shown in our supporting information file (Figure S4).

Forward synthesis: Initially 6-azido-N-(4-chlorophenyl)hexanamide **3** (Figure S5) was prepared from 6-bromohexanoic acid following Scheme 1 and according to the method mentioned in the literature.[5]

Table 2 — Results of the Docking of BSA, HSA and BMLN with SSAM-1

Protein-Name	PDB-ID	Docking Score SSAM-1 (kcal/mol)
BSA	4F5S	- 10.8
HSA	1AO6	- 9.4
BMLN	1W0Q	- 10.2

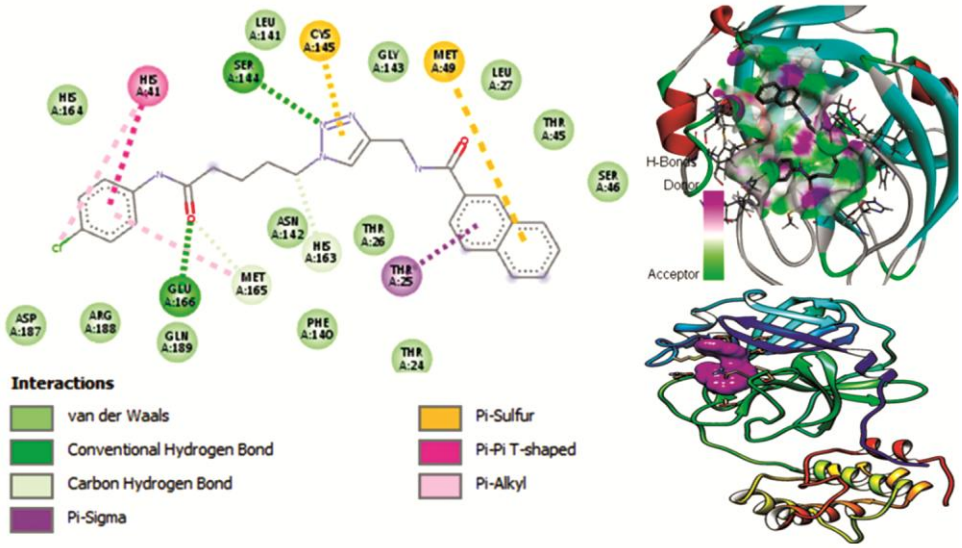

Fig. 3 — Docking Poses of SSAM-1 with 6LU7.

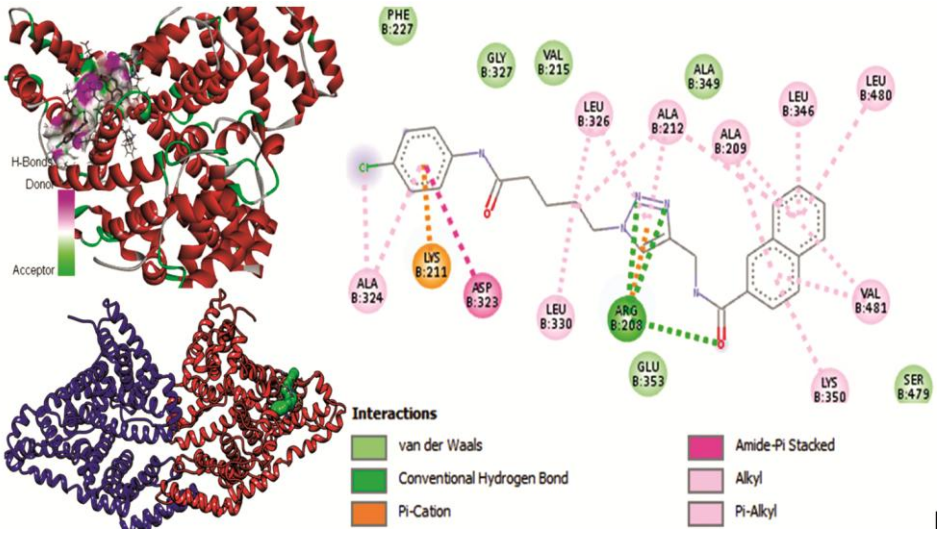

Fig. 4 — Docking Poses of SSAM-1 with 4F5S (BSA)

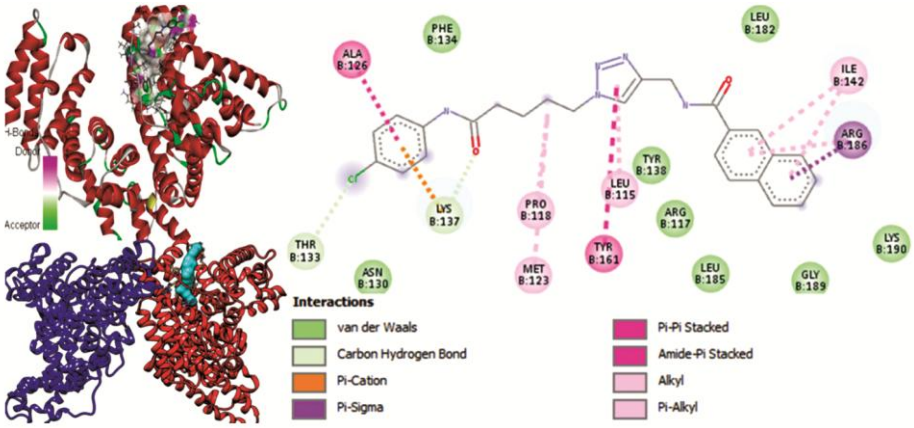

Fig. 5 — Docking Poses of SSAM-1 with 1AO6 (HSA)

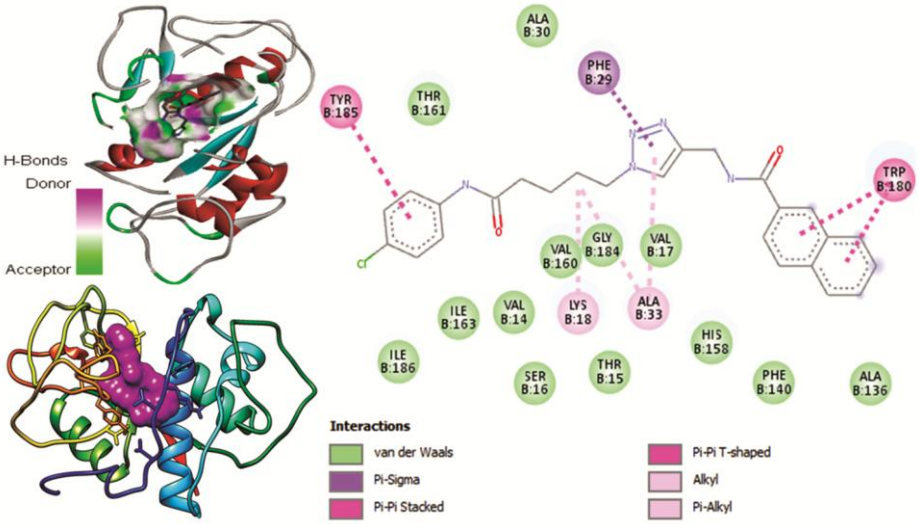

Fig. 6 — Docking Poses of SSAM-1 with 1W0Q (BMLN)

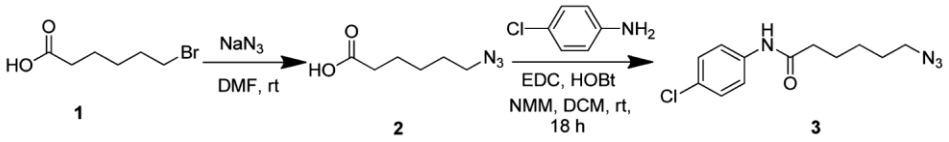

Scheme 1 — Synthesis of 6-azido-N-(4-chlorophenyl)hexanamide **3**

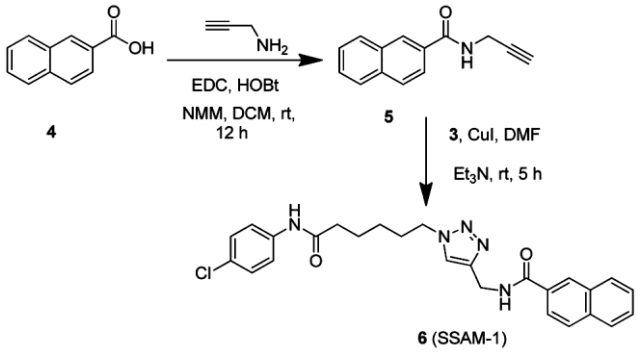

Scheme 2 — Synthesis of SSAM-1

Our desired molecule SSAM-1 (compound **6)** was prepared as per the Scheme 2 starting with commercially available 2-naphthoic acid. Alkyne naphthamide (**5**) (Figure S6) was prepared from 2-napthoic acid and propargylamine which further performed Click reaction with azide compound **3** in presence of CuI and afforded the desired compound **6** i.e. SSAM-1.

The structure of SSAM-1 was characterized with NMR (^{1}H and ^{13}C) (Figure S7, S8), FT-IR (Figure S9) and EI-MS (Figure S10).

Yield 0.248 g (51.8%). yellow solid. ^{1}H NMR (400 MHz, $(CD_3)_2SO$)), δ: 1.26 (m, 2H), 1.57 (m, 2H), 1.85 (m, 2H), 2.283 (t, 2H), 4.365 (t, 2H), 4.570 (s, 2H), 7.316 (d, 2H), 7.321 (d, 2H), 7.533 (s, 1H), 7.552 (s, 1H), 7.632 (d, 1H), 7.958 (d, 1H), 8.021 (d, 1H), 8.066 (d, 1H), 8.192 (s, 1H), 8.217 (d, 2H); ^{13}C NMR (100 MHz, (CD3)2SO), δ: 171.73, 169.02, 138.73, 130.39, 129.07, 128.70, 127.20, 126.72, 125.90, 125.81, 125.46, 123.26, 121.02, 36.65, 35.34, 31.22, 30.14, 26.02, 24.93.

IR(cm^{-1}): 3429.4 (amide N-H), 3287.42, 3141 (triazole C-H), 3054, 2934.53, 2864.03, 2096.36, 1634.21 (amide C=O) ,1538.9, 1494.74, 1424.66, 1303.79, 1235.14, 1206.44, 1135.71, 1052.32, 981.22, 835.35, 771.21, 734.13, 675.05, 557.89.

EI-MS: Found, m/z: 498.1102 $[M+Na]^+$. $C_{26}H_{26}ClN_2O_5Na$. Calculated, m/z: 498.96.

Steady-State Emission Studies at 298 K

Tryptophan (Trp) residues, whose excitation is performed at 290 nm[24,25], frequently found in the intrinsic fluorescence spectra of free BSA, HSA and BMLN. With the addition of an increasing concentration of the compound at 298 K in an aqueous phosphate buffer, the fluorescence emission maxima of two Trp residues for BSA (10 µM) rapidly decreased as well as moved from ~343 nm to ~340 nm (Fig. 7A). The similar phenomenon was seen for HSA as it was for BSA at 298 K and 290 nm (Fig. 7B); with the addition of the compound, the emission spectra of the single Trp residue (Trp 214) in free HSA (10 µM) were quenched as well as blue shifted. HSA shows emission maxima at approximately 338 nm, which gradually moved to the blue around 336 nm. The molecule disrupts the tryptophan microenvironment of serum albumins and binds with them, as evidenced by the decrease in fluorescence intensity in both cases (BSA/HSA). The blue shift indicates that the environment of the tryptophan residue becomes more hydrophobic or apolar with gradual addition of the compound. In the case for BMLN, the fluorescence emission intensity of the tryptophan residues also decreased with gradual addition of SSAM-1 molecule and the emission maxima shift towards longer wavelength, that is, a small red shift (335.4nm-337.6nm at 298K) was observed (Fig. 7C). This small red shift (of approx. 2 nm) indicates a decrease in hydrophobicity of the tryptophan microenvironment of BMLN.

Binding Data from Fluorescence Spectra

To find out the binding phenomena of SSAM-1 with the serum albumins and BMLN, the fluorescence emission intensity data for serum albumins and BMLN were analysed quantitatively by using the Stern−Volmer equation (eqn. 1).

$$F_0/F = 1 + K_{SV}[Q] = 1 + k_q\tau_0[Q] \quad \ldots (1)$$

The fluorescence intensities of serum albumin proteins and BMLN in the absence and presence of the quencher molecule (SSAM-1) represented by F_0 and F respectively, the Stern-Volmer quenching constant is K_{SV}, and the quencher SSAM-1 concentrations is [Q], k_q is the bimolecular quenching rate constant, $<\tau_0>$ is the average fluorophore lifetime

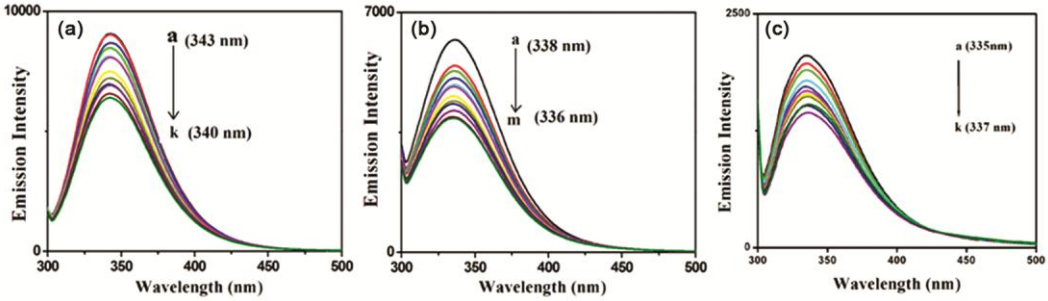

Fig. 7 — Room temperature fluorescence spectra of (A) Free BSA (10 µM) and its varying concentration of SSAM-1 in aqueous phosphate buffer (pH 7). Excitation wavelength = 290 nm; excitation and emission band pass = 10 nm and 5 nm respectively, (B) Free HSA (10 µM) and its varying concentration of SSAM-1 in aqueous phosphate buffer (pH 7). Excitation wavelength = 290 nm; excitation and emission band pass = 10 nm and 5 nm respectively. (C) Free BMLN (5 µM) and its varying concentration of SSAM-1in aqueous phosphate buffer (pH 7). Excitation wavelength = 290 nm; excitation and emission band pass = 10 nm and 5 nm respectively.

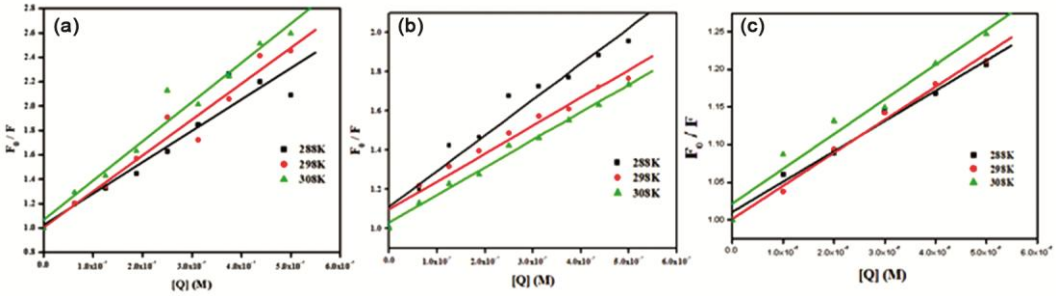

Fig. 8 — Stern Volmer plot of (A) Free BSA (10 µM) and its varying concentration of SSAM-1 in aqueous phosphate buffer (pH 7). Excitation wavelength = 290 nm; excitation and emission band pass = 10 nm and 5 nm respectively, (B) Free HSA (10 µM) and its varying concentration of SSAM-1 in aqueous phosphate buffer (pH 7). Excitation wavelength = 290 nm; excitation and emission band pass = 10 nm and 5 nm respectively. (C) Free BMLN (5 µM) and its varying concentration of SSAM-1in aqueous phosphate buffer (pH 7). Excitation wavelength = 290 nm; excitation and emission band pass = 10 nm and 5 nm, respectively.

Table 3 — Stern-Volmer quenching constant (K_{SV}) and bimolecular quenching constant (k_q) of the complex of SSAM-1 with both the serum albumins (BSA and HSA) and bromelain (BMLN) in aqueous buffer (pH 7) at 288 K, 298K and 308K.

Systems	Temperature (K)	Ksv (M^{-1})	Kq ($M^{-1}S^{-1}$)	R^2
BSA-SSAM-1	288	2.57×10^{6}	5.14×10^{14}	0.92
	298	2.94×10^{6}	5.89×10^{14}	0.96
	308	3.21×10^{6}	5.89×10^{14}	0.96
BMLN-SSAM-1	288	4.02×10^{5}	4.02×10^{13}	0.98
	298	4.39×10^{5}	4.39×10^{13}	0.99
	308	4.61×10^{5}	4.61×10^{13}	0.96
HSA-SSAM-1	288	1.81×10^{6}	3.61×10^{14}	0.95
	298	1.43×10^{6}	2.85×10^{14}	0.96
	308	1.41×10^{6}	2.81×10^{14}	0.99

in the absence of quencher SSAM-1. The value of $<\tau_0>$ for BSA and HSA is considered to be 5 nanoseconds[27] and that for BMLN is 10 nanoseconds[28]. All the fluorescence intensity data and area under the emission curve was used to determine F_0 and F as shown in Fig. 8. The K_{SV} and k_q values for different systems of serum albumins are summarized in Table 3.

The quenching interaction of the tryptophan fluorescence with the compound under investigation can occur via different mechanisms of which most common are static and dynamic quenching. Dynamic quenching is brought on by collisional interactions between the protein and the quencher, as opposed to static quenching, which is brought on by the formation of a stable complex between the protein and the quencher. The linearity of the Stern-Volmer equation can be used to describe both static and dynamic processes[29,30]. In our study, the nature of the Stern-Volmer plot (Fig. 8) for the interaction between

SSAM-1 with BSA, HSA and BMLN were found to be linear which indicated that only one quenching mechanism is operative. Moreover, the values of k_q obtained from the Stern–Volmer plot in case of BSA, HSA and BMLN were found to be much higher (in the order of 10^{13}-10^{14} $M^{-1}\cdot s^{-1}$) than the maximum scattered collision quenching constant (2×10^{10} $M^{-1}\cdot s^{-1}$) [26]. Hence, the quenching processes in all the proteins was expected to follow the static quenching mechanism.

For static quenching, the value of K_{SV} should decrease with increase in temperature. We found that only in case of HSA-SSAM-1 interaction, the K_{sv} value decreases with rise in temperature, but reverse effect occurred for BSA-SSAM-1 and BMLN-SSAM-1 interaction (Table 3). However, such anomalous behavior is not uncommon. Tong et al. had observed similar effect during the study of interaction of a hydrozone derivative with BSA[31]. Imbrahim et al. also had observed such effect during study of interaction of a synthesized derivative of indolone-N-oxide with HSA[32]. Also, Zhang et al. observed similar effect during the interaction of pyridoxine hydrochloride with BSA[33].

This apparent anomaly can be explained by considering Arrhenius equation. The bimolecular quenching constant is basically a rate constant and it increases with the increasing temperature. At higher temperatures, the protein-ligand complex becomes destabilized and its dissociation is favoured. If, at higher temperature the increase in the value of bimolecular quenching constant greatly outweighs the effect of destabilization of the complex, then the value of K_{SV} can increase with rise in temperature[34] for a static quenching[35,36].

The binding interaction between serum albumins and SSAM-1 can also be evaluated by using modified Scatchard equation,[25] shown as follows (eq. 2)

$$\log[(F_0\text{-}F)/F] = \log K_b + n \log[Q] \quad \ldots (2)$$

Where, where, F_0 and F represents the fluorescence intensities of BSA, HSA and BMLN in the absence and presence of quencher molecule (SSAM-1) respectively, K_b is the binding constant of all the protein-quencher complexes and 'n' is the number of binding sites. F_0 and F in all the cases of Fig. 9 being calculated considering the area under the emission curve of the fluorescence spectra. The double logarithmic plots of $\log[(F_0\text{-}F)/F]$ vs. $\log[Q]$ of the complexes BSA, HSA and BMLN with SSAM-1 system are presented in Fig. 9 respectively. The values of K_b and 'n' are listed in Table 4.

The binding constant values (K_b) for the interaction of SSAM-1 with BSA and BMLN are found to show similar trend. In these cases, the value of K_b decreases with rise in temperature. This indicates that SSAM-1 binds strongly with these proteins at lower temperature. This also supports the presence of static quenching. In case of static quenching, the protein-SSAM-1 complex is formed and at higher temperature the dissociation of the complex is favored and this leads to lowering of K_b value at higher temperature. Such trend is observed in many cases during interaction of small molecules with proteins[27,37]. However, reverse effect is observed for HSA-SSAM-1 interaction, where the binding constant increases with temperature. It signifies that SSAM-1 binds more strongly with HSA at higher temperature. This can be explained by considering the enthalpy and entropy factor.

Thermodynamic parameters and nature of interacting force

The thermodynamic parameters (ΔG, ΔH, ΔS) can be determined from the binding constant value using

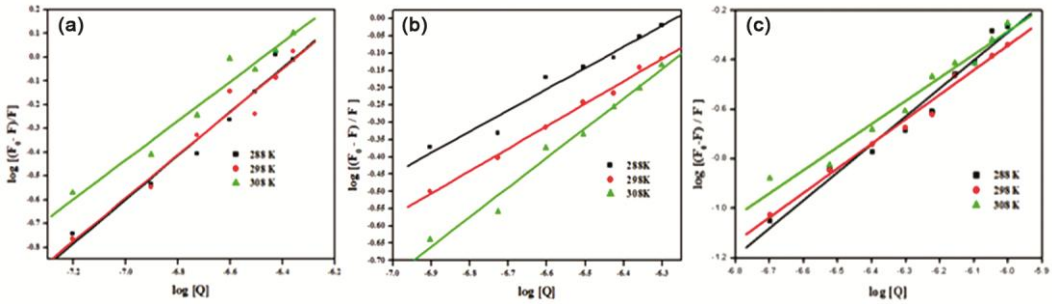

Fig. 9 — Double logarithmic plot/Scatchard plot of (A) Free BSA (10 µM) and its varying concentration of SSAM-1 in aqueous phosphate buffer (pH 7). Excitation wavelength = 290 nm; excitation and emission band pass = 10 nm and 5 nm respectively, (B) Free HSA (10 µM) and its varying concentration of SSAM-1 in aqueous phosphate buffer (pH 7). Excitation wavelength = 290 nm; excitation and emission band pass = 10 nm and 5 nm respectively. (C) Free BMLN (5 µM) and its varying concentration of SSAM-1in aqueous phosphate buffer (pH 7). Excitation wavelength = 290 nm; excitation and emission band pass = 10 nm and 5 nm respectively.

Table 4 — Binding constant (K_b) of the complex of SSAM-1 with both the serum albumins (BSA and HSA) and bromelain (BMLN) in aqueous buffer (pH7) and the corresponding number of binding sites (n) at 288K, 298K and 308K.

Systems	Temperature (K)	K_b (M^{-1})	n	R^2
BSA-SSAM-1	288	7.48×10^5	0.924	0.97
	298	5.77×10^5	0.907	0.95
	308	2.16×10^5	0.824	0.96
BMLN-SSAM-1	288	30.9×10^5	1.131	0.96
	298	4.1×10^5	0.993	0.98
	308	2.07×10^5	0.934	0.97
HSA-SSAM-1	288	6.88×10^3	0.612	0.96
	298	9.38×10^3	0.645	0.99
	308	1.78×10^5	0.856	0.99

Table 5 — Thermodynamic parameters of the complex of SSAM-1 with both the serum albumins (BSA and HSA) and bromelain (BMLN) in aqueous buffer (pH 7)

Systems	Temperature (K)	ΔG (kJ mol^{-1})	ΔH (kJ mol^{-1})	ΔS (J mol^{-1} K^{-1})
BSA-SSAM-1	288	-32.38		
	298	-32.87	-45.37	-44.05
	308	-31.46		
BMLN-SSAM-1	288	-35.81		
	298	-32.03	-100.36	-225.83
	308	-31.36		
HSA-SSAM-1	288	-21.16		
	298	-22.66	+119.01	+483.02
	308	-30.97		

the following equations,

$\Delta G = \Delta H - T\Delta S$ and $\Delta G = - RT \ln K_b$

Hence, $\Delta H - T\Delta S = -RT \ln K_b$

or, $\ln K_b = -\frac{\Delta H}{R\left(\frac{1}{T}\right)} + \Delta S$

Plot of $\ln K_b$ vs. (1/T) plot (Fig. 10) gives a straight line. From its slope and intercept, the value of change in enthalpy and entropy is calculated and the results are listed in Table 5. The negative value of Gibbs free energy in all cases indicates spontaneous binding of SSAM-1 with all the proteins (BSA, HSA and BMLN) at all the experimental temperatures. According to Subramanian and Ross[27], the signs of the values of enthalpy change and entropy change indicate different types of interaction as stated below-

$\Delta H < 0$, $\Delta S < 0$: van der Waals interaction and hydrogen bond formation.

$\Delta H > 0$, $\Delta S > 0$: hydrophobic interaction.

$\Delta H < 0$, $\Delta S > 0$: electrostatic interaction.

Hence from Table 5, we can conclude that the interaction of SSAM-1 with BSA and BMLN occurs mainly due to van der Waals interaction and hydrogen bond formation, but SSAM-1 interacts with HSA mainly via hydrophobic interaction.

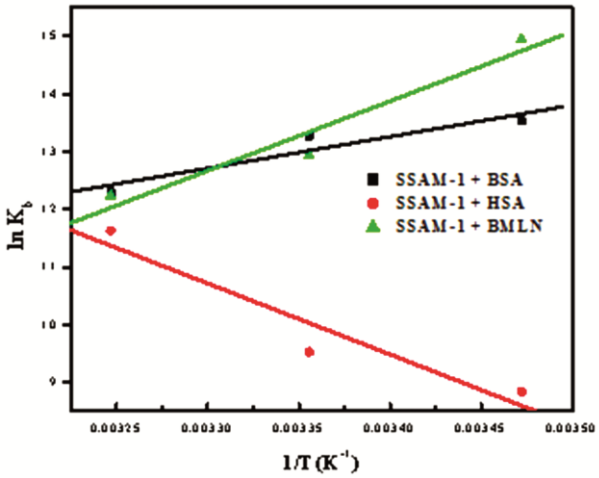

Fig. 10 — Plot of $\ln K_b$ against 1/T (K) of SSAM-1 complex with BSA, HSA and BMLN

ADME Prediction Results

The result from SWISS ADME of SSAM-1 came very satisfactory as it offers no violation from Lipinski's rule, Ghose rule, Egan rule and Muegge rule and it shows high gastrointestinal absorption as shown in Table 6 and is soluble in water as well, and it has a good bio-radar (Fig. 11a) which makes it a fair candidate as orally admissible drug molecule. In the boiled egg diagram (Fig. 11b) if the small circle

Table 6 — Results of the ADME prediction from SWISS-ADME of SSAM-1

Physicochemical Properties		Pharmacokinetics	
Formula	$C_{25}H_{24}ClN_5O_2$	GI absorption	High
Molecular weight	461.94 g/mol	BBB permeant	No
Num. heavy atoms	33	P-gp substrate	Yes
Num. arom heavy atoms	21	CYP1A2 inhibitor	Yes
Fraction Csp3	0.20	CYP2C19 inhibitor	Yes
Num. rotatable bonds	11	CYP2C9 inhibitor	Yes
Num. H-bond acceptors	4	CYP2D6 inhibitor	Yes
Num. H-bond donors	2	CYP3A4 inhibitor	Yes
Molar Refractivity	129.54	Log K_p (skin permeation)	–6.40 cm/s
TPSA	88.91 Å^2		
Lipophilicity		**Druglikeness**	
Log $P_{o/w}$ (iLOGP)	3.45	Lipinski	Yes; 0 violation
Log $P_{o/w}$ (XLOGP3)	3.83	Ghose	Yes
Log $P_{o/w}$ (WLOGP)	4.48	Veber	No; 1 violation: Rotors>10
Log $P_{o/w}$ (MLOGP)	3.29	Egan	Yes
Log $P_{o/w}$ (SILICOS-IT)	4.30	Muegge	Yes
Consensus Log $P_{o/w}$	3.87	Bioavailability Score	0.55

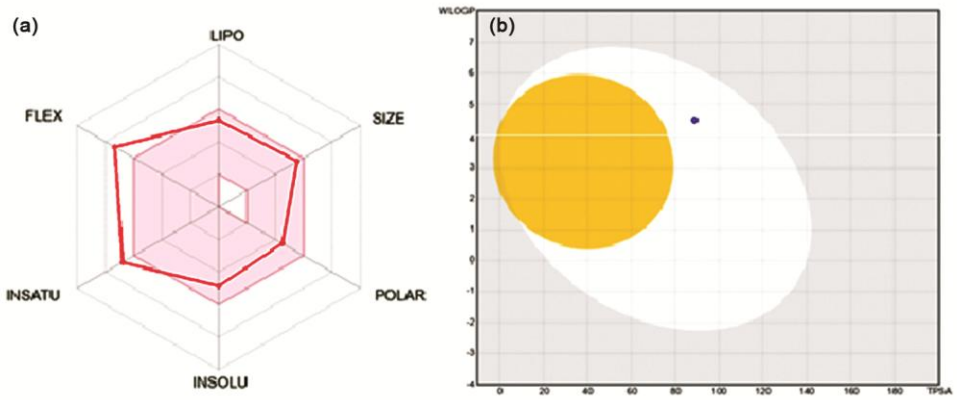

Fig. 11 — Bio-radar diagram (a) and Boiled egg diagram (b) of SSAM-1

appears over the white zone then it has high gastrointestinal absorption, the blue colour tells that it would be effluxed out or metabolised by poly glyco proteins. The circle is far from the yellow zone which means it will not pass through the blood brain barrier. So, the compound has a fair chance to act as a hydrocolloid.

It's log P value of 3.45 which is essential for showing drug like property (Table 6). The Total Polar Surface Area (TPSA) of SSAM-1 is also appropriate. From pKCSM server we predict the toxicity of SSAM-1 and found that it does not have any AMES or Renal toxicity (Table S1).

Conclusions

Novel 1,2,3-triazole-naphthamide compound SSAM-1 was designed using the concept of De novo drug design and synthesized using click reaction and later on the interactions of SSAM-1 with BSA, HSA and BMLN was examined utilizing steady state fluorescence investigations in aqueous phosphate buffer (pH7) at different temperatures. Spectroscopic methods were used to validate the compound's structure. Fluorescence experiments indicate that complexation (mainly via static quenching mechanism) with the compound HSA changed the microenvironment of the Trp residue(s) of BSA, HSA and BMLN. Strong binding affinity between proteins and ligands is indicated by the binding constant values, which is in10^3-10^5 orders. The experimental binding constant values matches well with that of the mostly common drug candidates. The thermodyamic parameters indicate spontaneous interaction between SSAM-1 with all the three proteins under the experimental conditions. The signs of enthalpy and entropy change indicate hydrophobic forces as the

major interacting forces for SSAM-1-HSA interaction while H-bonding and van der Waals forces as the primary interacting forces for SSAM-1 interacting with BSA and BMLN. Considering the in-silico studies the binding domain of HSA protein is probably the warfarin binding site and binding domain of BSA protein is probably the Naproxen binding site since these shows highest docking scores. The binding forces are also supplemented by the molecular docking. At this early stage of research, this binding analysis indicates that SSAM-1 molecule may act as a drug (as predicted from theoretical ADMET results) or a potential therapeutic candidate (due to binding with serum albumins) and the compound may be suitable for oral administration because of its binding interaction with BMLN. Thus, it can be further examined for its medicinal effectiveness in future.

Acknowledgments

This research was supported by the Science and Engineering Research Board (SERB), India. AM acknowledges SERB for research grant ref: EEQ/2019/000194. The authors are also thankful to the Presidency University, Kolkata for providing FRPDF research grant, laboratory and NMR facilities. The authors are grateful to the reviewers for their useful suggestions.

Declaration of competing interest

The authors declare that there are no conflicts of interest.

Supplementary Information

Supplementary information is available in the website http://nopr.niscpr.res.in/handle/123456789/58776.

References

1 Rotstein S H & Murcko M A, *J Com Aided Mol Des*, 7 (1993) 23.
2 Pakrashy S, Mandal P K, Dey S K, Choudhury S M, Alasmary F A, Almalki A S, Islam M A & Dolai M, *ACS Omega*, 7 (2022) 33408.
3 Kosa T, Maruyama T & Otagiri M, *Pharm Res*, 14 (1997) 1607.
4 Carter D C & Ho J X, *Adv Protein Chem*, 45 (1994) 153.
5 Paul S, Roy P, Sardar P S & Majhi A, *ACS Omega*, 4 (2019) 7213.
6 Albrecht C & Lakowicz J R, *Anal Bioanal Chem*, 390 (2008) 1223.
7 Ruan K, Li J, Liang R, Xu C, Yu Y, Lange R & Balny C, *Biochem Biophys Res Com*, 293 (2002) 593.
8 Colletti A, Li S, Marengo M, Adinolfi S & Cravotto G, *Appl Sci*, 11 (2021)8428.
9 Ramli A N M, Aznan T N T & Illias R M, *J Sci Food Agric*, 97 (2017) 1386.
10 Mynott T L, Luke R K J & Chandler D S, *Gut*, 38 (1996) 28.
11 De Sousa I P, Cattoz B, Wilcox M D, Griffiths P C, Dalgliesh R, RogersS & Schnürch A B, *Eur. J. Pharm. Biopharm*, 97 (2015) 257.
12 Paul S, Sepay N, Sarkar S, Roy P, Dasgupta S, Sardar P S & Majhi A, *New J Chem*, 41 (2017) 15392.
13 Sivakumar K, Xie F, Cash B M, Long S, Barnhill H N & Wang Q, *Org Lett*, 6 (2004) 4603.
14 Shi Y & Zhou C H, *Bioorganic & Med Chem Lett*, 21 (2011) 956.
15 15 Zhang W, Li Z, Zhou M, Wu F, Hou X, Luo H, Liu H, Han X, Yan G, Ding Z & Li R, *Bioorganic & Med Chem Lett*, 24 (2014) 799.
16 Rojas P L, Janeczko M, Kubiński K, Amesty Á, Masłyk M & Braun A E, *Molecules*, 23 (2018) 199.
17 Shaikh M H, Subhedar D D, Khan F A K, Sangshetti J N & Shingate B B, *Chinese Chem Lett*, 27 (2016) 295.
18 Trott O & Olson A J, *J Comp Chem*, 31 (2010) 455.
19 Krivov G G, Shapovalov M V & Dunbrack R L, *Pro Stru Fun Bioinfo*, 77 (2009) 778.
20 Wang J, Wang W, Kollman P A & Case D A, *J Am Chem Soc*, 222 (2001) U403.
21 Guex N & Peitsch M C, *Electrophoresis*, 18 (1997) 2714.
22 Gasteiger J & Jochum C, *J Chem Inf Comp Sci*, 19 (1979) 43.
23 Daina A, Michielin O & Zoete V, *Sci Rep*, 7 (2017) 42717.
24 Pires D E V, Blundell T L & Ascher D B, *J Med Chem*, 58 (2015) 4066.
25 Paul S, Ghanti R, Sardar P S & Majhi A, *Chem Heterocycl Compd*, 55 (2019) 607.
26 Paul S, Roy P, Das S, Ghosh S, Sardar P S & Majhi A, *ACS omega*, 6 (2021) 11878.
27 Sengupta P, Sardar P S, Roy P, Dasgupta S & Bose A, *J Photochem Photobiol B Biol*, 183 (2018) 101.
28 Li X, Yang Z & Peng Y, *New J Chem*, 42 (2018) 4940.
29 Eftink M R & Ghiron C A, *Anal Biochem*, 114 (1981) 199.
30 30 Ge Y S, Jin C, Song Z, Zhang J Q, Jiang F L & Liu Y, *Spectrochim Acta Part A Mol Biomol Spectrosc*, 124 (2014) 265.
31 Tong J Q, Tian F F, Li Q, Li L L, Xiang C, Liu Y, Dai J & Jiang F L, *Photochem & Photobiol Sci*, 11 (2012) 1868.
32 Ibrahim N, Ibrahim H, Kim S, Nallet J P & Nepveu F, *Biomacromolecules*, 11 (2010) 3341.
33 Zhang H, Huang X & Zhang M, *Mol Biol Rep*, 35 (2008) 699.
34 Ghosh N, Mondal R & Mukherjee S, *Langmuir*, 31 (2015) 8074.
35 Tian F F, Jiang F L, Han X L, Xiang C, Ge Y S, Li J H, Zhang Y, Li R, Ding X L & Liu Y, *J Phys Chem B*, 114 (2010) 14842.
36 Mondal P, Sengupta P, Pal U, Saha S & Bose A, *Spectrochim Acta Part A Mol Biomol Spectrosc*, 245 (2021) 118936.
37 Zhang J, Zhuang S, Tong C & Liu W, *J Agric F*, 61 (2013) 7203.